Applied Energy 224 (2018) 371–381

Contents lists available at ScienceDirect

Applied Energy

journal homepage: www.elsevier.com/locate/apenergy

Energy saving and economic analysis of a new hybrid radiative cooling system for single-family houses in the USA

Kai Zhang[a,d], Dongliang Zhao[b], Xiaobo Yin[b,c], Ronggui Yang[b], Gang Tan[a,*]

[a] Department of Civil and Architectural Engineering, University of Wyoming, Laramie, WY 82071, USA
[b] Department of Mechanical Engineering, University of Colorado, Boulder, CO 80309, USA
[c] Materials Science and Engineering Program, University of Colorado, Boulder, CO 80309, USA
[d] College of Urban Construction, Nanjing Tech University, Nanjing 210009, China

HIGHLIGHTS

- Novel hybrid Radiative cooled-Cold storage cooling (RadiCold$_{hc}$) system is proposed.
- Energy and economic analysis are investigated on a highly insulated two-story house.
- RadiCold$_{hc}$ system will save annual cooling electricity consumption by 26–46%.
- Maximum incremental costs are \$50.0/m^2–\$78.9/m^2 for an 8-year simple payback period.

ARTICLE INFO

Keywords:
Radiative cooling
Cold energy storage
Energy saving
Building simulation
Residential buildings

ABSTRACT

Radiative cooling has received much attention as it generates "free" cooling to buildings and helps reduce energy consumption of mechanical air conditioning systems. However, most current radiative cooling materials either work for nighttime (nocturnal) cooling only or have high cost issues. A novel scalable-manufactured randomized glass-polymer hybrid metamaterial coated with silver has recently been developed and reported a 110 W/m^2 cooling power on daily average. This metamaterial potentially provides passive cooling for both nighttime and daytime. Proposed is a hybrid diurnal radiative cooled-cold storage cooling system using this metamaterial for air conditioning purposes in single-family houses. Because single-family houses have a relatively low cooling load but high ratio of roof area to floor area, they are excellent end users of the hybrid radiative cooled-cold storage cooling system. The potential energy savings of the hybrid radiative cooled-cold storage cooling system in a typical two-floor single-family house with floor area of 204 m^2 have been modeled using EnergyPlus for four locations in the U.S., including Orlando, FL, San Diego, CA, San Francisco, CA, and Denver, CO. In comparison with the electricity consumption of a split air conditioner alone, the hybrid radiative cooled-cold storage cooling system could save annual cooling electricity by 26% to 46% for the modeled locations, under a restriction of 8-year payback period. The corresponding simple payback periods for adoption of the hybrid radiative cooled-cold storage cooling system fall in a range of 4.8–8.0 years and the maximum acceptable incremental costs are \$50.0/m^2–\$78.9/m^2. The diurnal working hybrid radiative cooled-cold storage cooling system may provide a cost-effective solution for radiative cooling technology in residential building applications.

1. Introduction

As a passive cooling technology, radiative cooling surface transfers heat to sky by infrared radiation whenever the effective sky temperature is lower than the radiative surface temperature [1–4]. Although the radiative cooling technique has been developed for many years [5–9], the application has been limited to nighttime due to solar absorption of most materials in the daytime [10–14]. With the development of micro/nanotechnologies, daytime radiative cooling has become possible, and applications of diurnal cooling to buildings could be realized [15,16]. In particular, Zhai et al. [17] has recently developed the radiative cooling film, of a randomized, glass-polymer hybrid metamaterial with silver coating, and characterized with effectively rejecting solar irradiance and strongly emitting in the infrared. This film can be scalable-manufactured at relatively low-cost. It provides high technical and economic potential for the development of diurnal radiative cooling

* Corresponding author.
E-mail address: gtan@uwyo.edu (G. Tan).

https://doi.org/10.1016/j.apenergy.2018.04.115
Received 10 December 2017; Received in revised form 1 March 2018; Accepted 30 April 2018
Available online 11 May 2018

Nomenclature

A_S area of the radiative cooling surface (m^2)
AIC_{max} maximum acceptable incremental cost per unit area of radiative cooling surface ($/$m^2$)
$ASPP$ Acceptable simple payback period (year)
C_{Radi} cost of the RadiCold system ($)
C_{RSAC} cost of the reduced-size split air conditioner in $RadiCold_{hc}$ system ($)
C_{RC} cooling capacity for a of RadiCold module (kW)
C_{SACL} cost of the split air conditioner lonely ($)
c_p specific heat capacity of water (J/kg·K)
$CL_{avg\text{-}hour}$ average hourly cooling load (kW)
S_{RSAC} size of reduced-size split air conditioner (kW)
S_{SACL} size of split air conditioner lonely (kW)
$E_{Radi\text{-}hc}$ cooling electricity consumption of the $RadiCold_{hc}$ system (kWh)
E_{SACL} cooling electricity consumption of the split air conditioner lonely (kWh)
h_f forced convection component of radiative cooling surface ($W/m^2 \cdot K$)
h_n natural convection component of radiative cooling surface ($W/m^2 \cdot K$)
h_{RS} convective heat transfer coefficient over the radiative cooling surface ($W/m^2 \cdot K$)
I_{sol} incident solar radiation (W/m^2)
N number of RadiCold modules employed in the residential building
P perimeter length of radiative cooling surface (m)
P_E price of electricity ($/kWh)
q_{conv} convection heat transfer between radiative cooling surface and ambient air (W/m^2)
q_{RS} net radiative cooling power (W/m^2)
q_{rad} heat transfer between radiative cooling surface and sky (W/m^2)
q_{sol} solar radiation absorbed by the radiative cooling surface (W/m^2)
R_f roughness multiplier of radiative cooling surface
RSAC reduced-size split air conditioner
SACL split air conditioner lonely
SPP simple payback period (year)
$t_{charging}$ total charging time (s)
T_{amb} ambient air temperature (K)
T_d ambient dewpoint temperature (K)
T_{sky} effective sky temperature for longwave radiation (K)
T_{surf} temperature of radiative cooling surface (K)
$T_{w,\tau}$ RadiCold module water temprature of current time step (K)
$T_{w,\ \tau\ +1}$ RadiCold module water temperature of next time step (K)
T_w average water temperature in RadiCold module (K)
ΔT_{tank} variation of the temperature in the tank (K)
V volume of water in the RadiCold module (m^3)
V_{tank} volume of tank (m^3)
V_z local wind speed (m/s)
W_f wind direction modifier

Greek letter

α surface tile angle
ε_{sky} average spectral and directional longwave emissivity/absorptivity of the atmospheric
ε_{surf} radiative cooling surface emittance
η efficiency of discharging
λ absorption coefficient
ρ_w density of water (kg/m^3)
ρ_{surf} solar absorption rate of the radiative cooling surface
σ Stefan-Boltzmann constant ($J/(m^2 \cdot s \cdot K^4)$)
$\Delta\tau$ length of the time step (s)

systems for building applications. Direct thermal measurement of the radiative cooling film demonstrated approximately 110 W/m^2 cooling power on a daily average in hot weather [17].

Various strategies have been proposed utilizing the radiative cooling technology in buildings, including passive systems directly applying selective-emittance material for roofs, and active systems such as water based, air based, and hybrid systems (Fig. 1) [2,4].

The water based cooling systems can be categorized into two forms: open loop [18–22] and closed loop [23–26]. The open loop water system commonly consists of a shallow rooftop pond, where the heat is

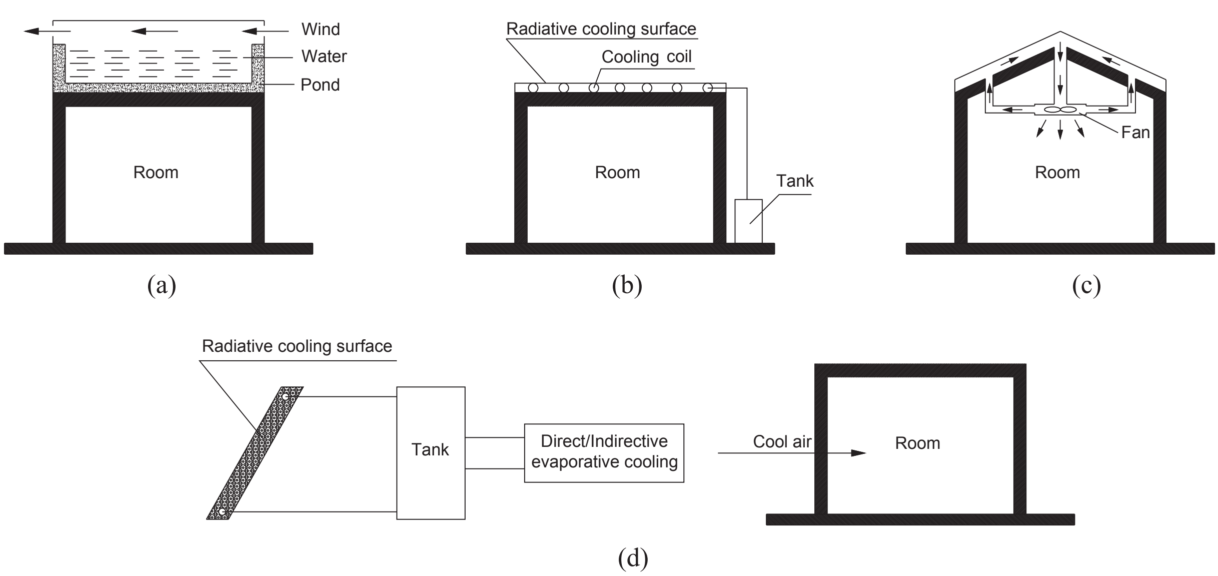

Fig. 1. Sketch of active radiative cooling systems: (a) water based system (open loop); (b) water based system (closed loop); (c) air based system; and (d) hybrid system.

transferred to the surrounding ambient by convection, radiation, and evaporation from the roof through the water in the rooftop pond. The closed loop water system differs from the open loop system because it uses water as the heat transfer fluid and the heat is dissipated by a flat-plate cooling radiator. Raeissi and Taheri [22] indicated that application of the open loop water based system can reduce the cooling load of the air conditioner by 52% in summer for a 140.6 m^2 single-story house in Iran. The air based system has the advantage of providing instantaneous cooling to building spaces during nighttime using a fan or driven by buoyancy force [27,28]. Mihalakakou et al. [29] studied the performance of an air based system for a rehabilitated historical industrial building with a 98 m^2 radiator. The results showed that their proposed system can provide daily useful cooling energy of 29.7–55.8 Wh/m^2 for clear sky and 26.7–44.9 Wh/m^2 for cloudy sky, based on the radiator's area. Khedari et al. [30] developed four types of roof radiators and applied them to air based system for a school solar house. During nighttime, their experiments showed the temperature of roof radiators could be 1–6 °C lower than the ambient air temperature under the weather condition in Thailand. Although the air based system is relatively simpler and cheaper, it is difficult to integrate with buildings [2]. Due to the requirement of a thin air channel and a large radiative cooling surface area, the air based system is more suitable for the detached house or the top floor of the multi-story building.

In literature, there are two kinds of hybrid systems; that is, as an integrated system of (1) the nocturnal radiative cooling with other energy-related system or (2) an air based system with a water based system [31–33]. Eicker and Dalibard [32] studied a hybrid system comprising photovoltaic radiators and building thermal mass embedded phase-change material for latent heat storage for a residential building located in Spain. Their work showed that the average nighttime cooling power of the hybrid system was about 40–45 W/m^2, and the cold water generated by this hybrid system can be used for direct cooling of an radiant floor or ceiling. Parker et al. [34,35] evaluated two hybrid systems, called WhiteCap and NightCool, for a single-family house with a roof area of 225 m^2. The results showed that 30–60% of annual cooling loads can be carried by WhiteCap in California and 46% cooling loads of June through September can be taken care of by NightCool in Florida. Parker et al. [35] also calculated the coefficient of performance (COP) of NightCool system in a typical cooling season (June to September), and the COPs were 10.9 for Tampa, FL and 26.0 for Baltimore, MD, respectively. Previous studies of the water based system, air based system, and hybrid system were for nocturnal radiative cooling technologies due to solar heating effect in the day. In addition, since the previous work was mostly focused on evaluating the energy savings from radiative cooling, there lacks of a thorough economic analysis for implementing radiative cooling into buildings.

The development of micro/nanotechnologies has brought on great opportunities to the radiative cooling technologies. Recent researches on the wavelength-selective emittance material or coating showed that advanced nanophotonic materials could lead radiative cooling to as much as 5 °C below the ambient temperature under direct sunlight [36–39]. This is a milestone break-through for radiative cooling technology and now radiative cooling can continuously produce cold energy throughout both daytime and nighttime. Fernandez et al. [4] proposed a hybrid system based on a nanophotonic material, in which a cold water tank stores cold energy generated by the nanophotonic material based radiative cooler while the cold water can be used as supplemental cooling source for a chiller. Their modeling results showed this hybrid system could save 45–68% cooling electric energy for medium-size office buildings compared to the conventional variable air volume (VAV) system in five U.S. locations, including fan power savings from converting the VAV system to a radiant cooling system. Their allowable incremental costs for 5-year simple payback period varied from \$2.5 to \$6.25 per square meter of the radiative cooling surface area by upgrading a nighttime radiative cooling product to a nanophotonic material based radiative cooler. However, it is difficult to achieve such low incremental cost when implementing nanophotonic material based radiative cooling technology. Currently, the advanced nanophotonic materials are expected to have limited applications, particularly due to their high cost and difficulties in mass production [4]. Table 1 summarizes the challenges that existing radiative cooling systems face for wide application in buildings.

Recently, the metamaterial reported by Zhai et al. [17] has been demonstrated with preferably diurnal cooling capacity and low-cost roll-to-roll manufacturing potential. A **h**ybrid **Radi**ative cooled-**Cold** storage **c**ooling (RadiCold$_{hc}$) system is proposed in this work for single-family houses, which have relatively low cooling load per unit floor area but high ratio of roof area to floor area. Considering that the most common cooling system employed in the U.S. single-family houses is the split air conditioner [40], our proposed RadiCold$_{hc}$ system consists of a RadiCold subsystem and a reduced-size split air conditioner (RSAC). A typical two-floor single-family house, with floor area of 204 m^2, has been modeled for evaluating the performance of the RadiCold$_{hc}$ system and the cost/benefit of the system using EnergyPlus for four U.S. locations, including Orlando, FL, San Diego, CA, San Francisco, CA, and Denver, CO.

2. Methodology

2.1. Proposed RadiCold$_{hc}$ system

Fig. 2 shows the proposed RadiCold$_{hc}$ system for residential buildings. There are two major subsystems in the RadiCold$_{hc}$ system: (1) a RadiCold subsystem, consisting of cold energy collectors (i.e., RadiCold modules) laminated with metamaterial based radiative cooling film on the top of water channels (see Fig. 3) and a cold-water storage tank connected with pipe network for space cooling whenever allowable; and (2) a RSAC, providing complimentary cooling capacity. This RadiCold$_{hc}$ system has three operation modes as described in Table 2.

The proposed RadiCold$_{hc}$ system not only can be installed in new

Table 1
Summary of different radiative cooling systems from literature [2,4,15]

System	Advantages	Disadvantages
Water based system	• Desirable performance under favorable climate conditions • Little effects of building orientation (open looped) • Retrofitted with a low cost (closed looped)	• Nocturnal cooling only • Roof should support the pond with a load of 200–400 kg/m^2 (open looped) • Water consumption (open looped) • Must be laid on a flat or slightly pitched roof (closed looped)
Air based system	• Low cost • No freeze and leakage	• Nocturnal cooling only • Poor building integration • Lower performance
Hybrid system	• Good performance • Multiple system combination	• Nocturnal cooling only
Selective emittance material or coating	• Nocturnal and diurnal cooling • Potential to integrate with existing building	• High cost • Difficult for mass production

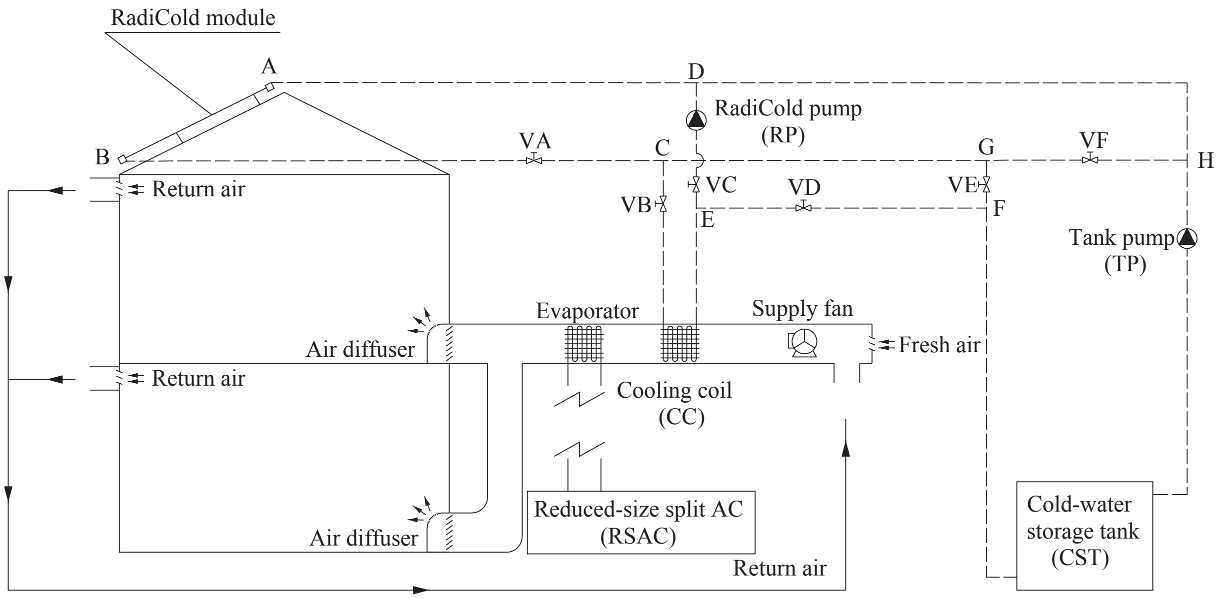

Fig. 2. Sketch of RadiCold$_{hc}$ system (labels A, B…, and H are the intersections of pipes, and labels VA, VB…, and VF are the valves).

construction buildings, but also can be used to retrofit existing single-family houses because the RadiCold subsystem works independently to the split air conditioner. There will be minimal disturbance to the existing split air conditioner system in single-family houses as the integration can be done by installing an extra cooling coil (CC) and no additional upgrades to the existing air distribution system would be required.

2.2. Theoretical model

Simulation has been conducted using the whole building simulation software EnergyPlus, which has models of split air conditioner and cooling coil [41]. Customized heat transfer models for the RadiCold module have been developed in this work. As shown in Fig. 3, the radiative cooling surface comprises the novel scalable-manufactured randomized glass-polymer hybrid metamaterial. The RadiCold module is well insulated (5 cm polyisocyanurate rigid foam insulation) at the four sides and the bottom and thus minimum heat losses through other surfaces except the top radiative cooling surface. The parallel water channels are made of polycarbonate panel as the polycarbonate panel has good long-term durability for outdoor applications (e.g., greenhouses). In this work, for the convenience of installation and problem simplification, the dimension of the RadiCold module is determined at 1.0 m^2 (1.0 m × 1.0 m) with an average cooling capacity of approximately 0.1 kW.

As shown in Fig. 3(a), the heat balance of the radiative cooling surface can be written as,

$$q_{RS} = q_{conv} + q_{rad} + q_{sol} \tag{1}$$

where q_{RS} is the net radiative cooling power of the radiative cooling surface; q_{conv} is the convective heat gain of the radiative cooling surface from ambient air; q_{rad} is the heat transfer rate between the radiative cooling surface and sky through infrared radiation; and q_{sol} is the solar radiation absorbed by the radiative cooling surface.

Convective heat loss could be impacted by wind speed, flow regime, surface orientation and roughness, etc. [42]. The inappropriate models will cause more than 10% error in the convective heat transfer coefficient [43]. The TRAP algorithm has been adopted in this study to calculate the convection heat transfer rate [44,45].

In the TRAP algorithm, q_{conv} can be expressed as,

$$q_{conv} = h_{RS}(T_{surf} - T_{amb}) \tag{2}$$

where h_{RS} is the convective heat transfer coefficient of the radiative cooling surface; T_{amb} is the ambient air temperature; and T_{surf} is the radiative cooling surface temperature.

The convective heat transfer is composed of forced convection and natural convection,

$$h_{RS} = h_f + h_n \tag{3}$$

where h_f is the forced convection heat transfer coefficient; and h_n is natural convection coefficient.

Forced convection heat transfer coefficient is given by [44],

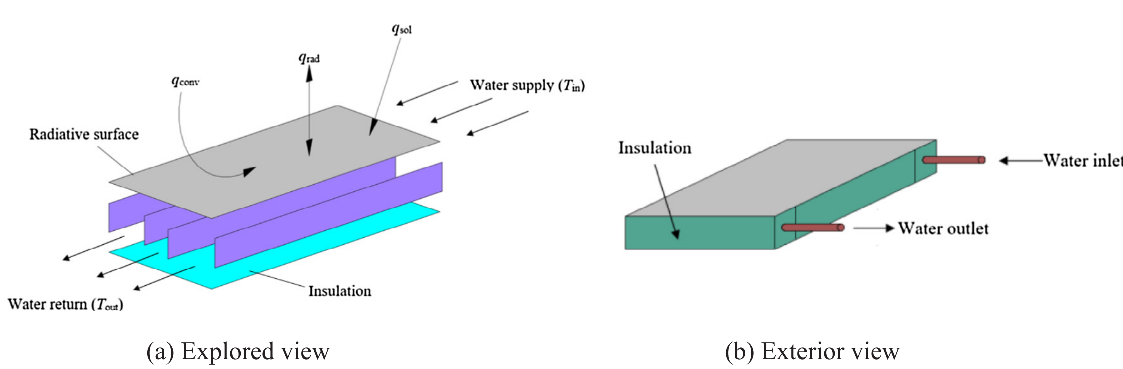

Fig. 3. Sketch of the RadiCold module.

Table 2
List of operation modes of the $RadiCold_{hc}$ system.

Modes	Loops	Valves open	Operation
Direct space cooling	A-B-C-CC-E-RP-D-A	VA, VB, and VC	• The cooling power of RadiCold subsystem is the same as or lower than the space cooling demand and no cold energy is stored in the tank • The radiative cooling energy generated by RadiCold modules is directly used to cool space through the cooling coil • The RSAC runs in space cooling mode to provide complimentary cooling to the space if the cooling power of RadiCold subsystem is lower than the space cooling load
Combined space cooling and cold storage charging	A-B-C-CC-E-F-CST-TP-H-D-A	VA, VB, and VD	• The space cooling load is lower than the cooling power of the RadiCold modules • Part of the cold energy produced by the RadiCold subsystem is used to cool the space through the cooling coil • Remaining portion of the cold energy is charged into the cold-water storage tank • Only the RadiCold subsystem runs while the RSAC is off
Cold storage for space cooling	C-CC-E-F-CST-TP-H-G-C	VB, VE, and VF	• The cold energy stored in the tank is used to cool the space • Water from the RadiCold subsystem is unavailable for space cooling or cold energy storage

$$h_f = 2.537 W_f R_f \left(\frac{PV_z}{A_S}\right)^{1/2} \tag{4}$$

where W_f is the wind direction modifier; R_f is the roughness multiplier of radiative cooling surface; P is the perimeter length of radiative cooling surface; V_z is the local wind speed; and A_S is the area of the radiative cooling surface.

Natural convection heat transfer coefficient is given by [45],

$$h_n = \begin{cases} \frac{9.482\,|T_{surf}-T_{amb}|^{1/3}}{7.238-|\cos\alpha|} & (T_{surf} < T_{amb}) \\ \frac{1.810\,|T_{surf}-T_{amb}|^{1/3}}{1.382+|\cos\alpha|} & (T_{surf} > T_{amb}) \end{cases} \tag{5}$$

where α is the surface tilt angle.

The solar energy absorbed, q_{sol}, can be calculated by,

$$q_{sol} = -\lambda I_{sol} \tag{6}$$

where λ is absorption coefficient, 0.04 in this work for the metamaterial-based radiative cooling surface [17]; and I_{sol} is the incident solar radiation.

Following the existing common method [32], the net radiative heat exchange between a body with emissivity ε_{surf} to the sky is given by,

$$q_{rad} = \sigma\varepsilon_{surf}(T_{surf}^4 - T_{sky}^4) \tag{7}$$

where σ is the Stefan-Boltzmann constant, $5.67 \times 10^{-8}\,W/m^2K^4$; ε_{surf} is the emittance of the radiative cooling surface, 0.93 for the metamaterial-based radiative cooling surface [17]; and T_{sky} is the effective sky temperature.

In order to relate the effective sky temperature and the ambient dry bulb temperature, the concept of effective sky emissivity is defined as a grey emitter with the same temperature as the ambient temperature [34],

$$T_{sky} = \varepsilon_{sky}^{1/4} T_{amb} \tag{8}$$

The atmospheric emissivity has great effects on the performance of the radiative cooling. During past decade years, noticeable efforts have been devoted in estimating the spectral and directional longwave emissivity/absorptivity of the atmosphere (ε_{sky}) [46–49]. Under clear sky condition, Berdahl and Martin [47] developed a model to relate the effective emissivity of sky (ε_{sky}) to ambient dew point temperature as follows,

$$\varepsilon_{sky} = 0.711 + 0.56(T_d/100) + 0.711(T_d/100)^2 \tag{9}$$

where T_d is the ambient dewpoint temperature.

Fig. 4 shows the comparison of the model predicted cooling power against the experimental data tested in the U.S. state of Arizona [17]. The existing radiative cooling models as given above represent the cooling power variation trend although there are some discrepancies.

In the RadiCold module, as shown in Fig. 3, water flows in the channels and transfers heat to the colder RadiCold cooling surface (50 µm metamaterial-based film) through a 0.5-mm-thick polycarbonate wall. Ignoring the thermal capacity and thermal resistance of the RadiCold cooling surface and the polycarbonate, the water temperature in the RadiCold module can be calculated for each time step,

$$\rho_w c_p V \Delta T_w = -q_{RS}\Delta\tau \tag{10}$$

Thus,

$$T_{w,\tau+1} = T_{w,\tau} - \frac{q_{RS}\Delta\tau}{\rho c_p V} \tag{11}$$

where ρ_w is the density of water; c_p is the specific heat of water; V is the volume of water in the RadiCold module; ΔT_w is the average water temperature change in the RadiCold module for a time step; $\Delta\tau$ is the length of the time step; $T_{w,\tau+1}$ is the RadiCold module water temperature at the next time step; and $T_{w,\tau}$ is the RadiCold module water temperature at the current time step.

3. Building simulation for $RadiCold_{hc}$ system

3.1. Building specification

To analyze the energy saving potential, a typical two-floor single-family house model (see Fig. 5) originated from the U.S. Department of

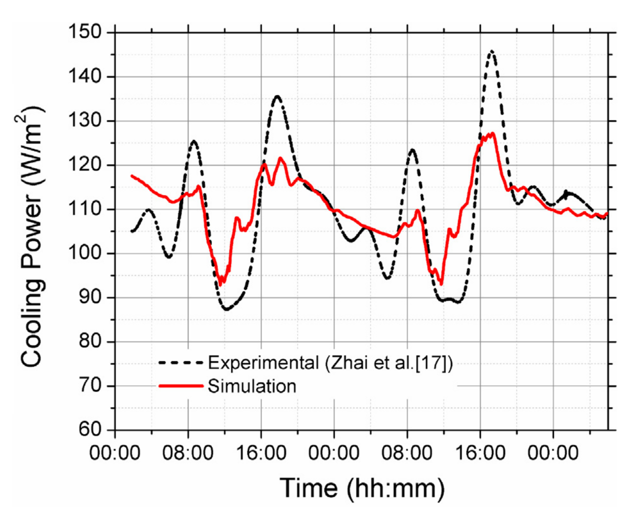

Fig. 4. Comparison of model predicted cooling power and measured cooling power for the metamaterial-based radiative cooling surface developed by Zhai et al. [17].

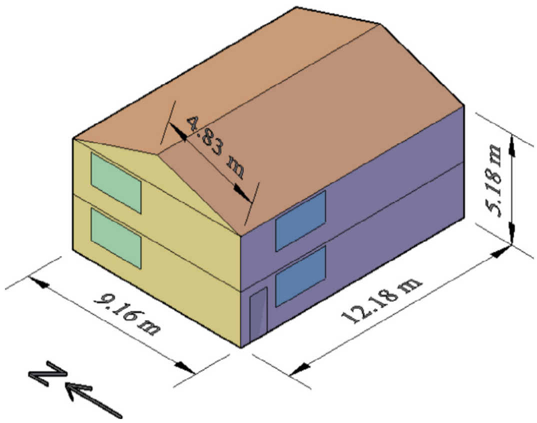

Fig. 5. Sketch of the single-family house model.

Table 3
Details of the model building.

Items	Parameter	
Floor area	204 m^2	
Roof area	118 m^2	
Air conditioning device	Split air conditioner	
Indoor air temperature setting (cooling)	24 °C	
Occupants	3	
Window-wall ratio	10%	
Insulation	Orlando	Wall: R13
		Roof: R38
	San Diego	Wall: R13
		Roof: R38
	San Francisco	Wall: R13
		Roof: R38
	Denver	Wall: R13 + R3.8
		Roof: R38

Energy (DOE) building energy codes program (2012 IECC) [50] is used, for which the details are given in Table 3. Simulation analysis has been conducted for four locations in the USA, including Orlando, FL (for hot-humid climate), San Diego, CA (for hot-dry climate), San Francisco, CA (for marine climate), and Denver, CO (for cold climate).

3.2. Optimization of the RadiCold$_{hc}$ system

In literature, most of the previous studies focused on energy savings of radiative cooling systems. However, both the energy saving and the cost should be simultaneously evaluated for a newly proposed radiative cooling system/technique in order to comprehensively understand its application potential in buildings. To balance energy saving and economic feasibility, we introduce an optimization method for sizing the RadiCold$_{hc}$ system, which includes determining the number of RadiCold modules, the cold storage tank volume, the circulation pump and the pipe network size. The overarching goal of the RadiCold$_{hc}$ system sizing method is to obtain an economically feasible system with good energy saving.

As shown in Fig. 6, the optimization process can be written as below,

$$\begin{cases} \min SPP = f(N_i, V_{tank,i}, P_{pump,i}, S_{RSAC,i}, S_{SACL}, P_E) \\ s.\ t.\ \ N_i \leqslant N_{initial} \\ N_{i+1} = N_i - 1 \\ SPP \leqslant ASPP \end{cases} \tag{12}$$

where *SPP* is the simple payback period of implementing RadiCold$_{hc}$ system but without accounting for the time value of money; *N* is the number of RadiCold modules; V_{tank} is the tank volume; S_{RSAC} is the size of RSAC; S_{SACL} is the size of split air conditioner lonely (SACL); P_E is the price of electricity; *f* is a function of *N*, V_{tank}, S_{RSAC}, S_{SACL}, and P_E; *i* is the i^{th} of iteration; subscript "initial" refers to the initial value; and *ASPP* is the acceptable simple payback period which is defined as the accepted period of time by proprietor to reach the break-even point of an

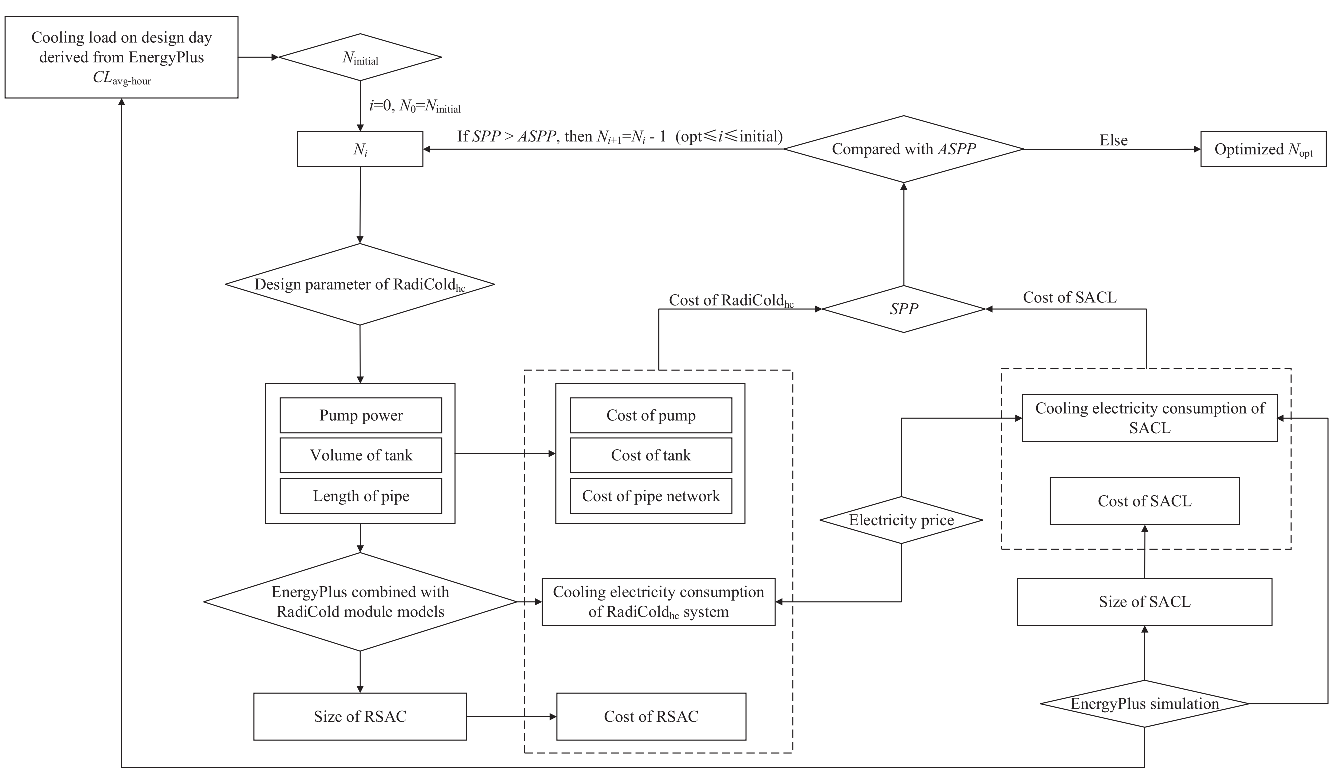

Fig. 6. Flow chart for optimizing the size of RadiCold$_{hc}$ system.

Table 4
Major component cost of the $RadiCold_{hc}$ system except RadiCold module [51].

No	Component	Average cost (including labor and material)
1	Tank	\$134.2/m^3
2	Pipe network	\$2.5/m
3	Plastics pump	\$1.7/W
4	Cooling coil	\$83.2/kW
5	Split air conditioner	\$404.5/kW

investment.

The optimization process starts from pre-sizing the RadiCold subsystem, and then the system is further evaluated based on the pre-sized RadiCold subsystem to satisfy the specified simple payback period criteria. This work uses 8-year as the threshold for *ASPP* considering the residential split air conditioner generally has a lifespan of 10–16 years (e.g., outside unit 10–16 years and inside unit 14–18 years) while the lifespan of the RadiCold subsystem is estimated more than 10 years.

The average hourly cooling load on the "design" day (i.e., July 21st for Orlando and Denver, and August 21st for San Diego and San Francisco [50]) is adopted to pre-size the $RadiCold_{hc}$ system. Taking the average hourly cooling load as the design cooling load can result in a RadiCold module number not too far from the optimized number, which may reduce the iteration process. Therefore, the initial number of RadiCold modules is given as,

$$N_{initial} = \frac{\sum_{i=1}^{24} CL_{avg-hour}}{24C_{RC}} \tag{13}$$

where $CL_{\text{avg-hour}}$ is the hourly cooling load in design day; and C_{RC} is the cooling capacity of single RadiCold module.

With average hourly cooling load ($CL_{\text{avg-hour}}$) derived from EnergyPlus simulation, the initial number of RadiCold modules (N_{initial}) can be calculated from Eq. (13). The pump power and length of pipes are determined by the cooling capacity of RadiCold subsystem (i.e., number of RadiCold modules). The volume of the cold storage tank can be sized according to the maximum requirement of cold storage. In this study, it has been simplified so that most cold energy would be charged to the cold storage tank during 0:00 to 5:00 in the cooling season. Tank volume can be calculated by Eq. (14) with an estimated cooled down temperature of 8 °C for the tank water during the charging period of 5 hours, while the cold storage efficiency is given at 90%.

$$\eta C_{RC} N_i t_{charing} = c_p \rho_w V_{tank,i} \Delta T_{tank} \tag{14}$$

where η is the efficiency of discharging; t_{charging} is the total charging time; and ΔT_{tank} is the effective usable temperature difference of water in the tank between ending and starting of the charging period.

However, the pre-sized $RadiCold_{hc}$ system could be oversized or the cost of the system might be too high to pass the economic threshold (e.g., *ASPP*). The *SPP* is an effective index to evaluate the feasibility of an investment or project, and a longer *SPP* is typically not desirable for investment position. The *SPP* is incorporated into the optimization of $RadiCold_{hc}$ system while the cost of the system is based on market retail price, construction cost estimation resource, and engineering estimation [51]. The *SPP* can be calculated by Eq. (15), in which the cost of pre-sized $RadiCold_{hc}$ system (see Fig. 6) can be derived from the calculated component costs and the electricity price (P_E) is applied. Then, the *SPP* may be recalculated using the iterative algorithm if *SPP* is higher than *ASPP*. The iteration will stop when the calculated *SPP* is the first time less than *ASPP*. Finally, the optimum number of RadiCold modules is obtained (N_{opt}). In this work, the 8-year threshold is used as the *ASPP* for sizing the $RadiCold_{hc}$ system [4].

The simple payback period can be calculated by,

$$SPP = \frac{C_{Radi} + C_{RSAC} - C_{SACL}}{(E_{SACL} - E_{Radi-hc})P_E} \tag{15}$$

where E_{SACL} is the annual cooling electricity consumption of SACL; $E_{\text{Radi-hc}}$ is the annual cooling electricity consumption of the $RadiCold_{hc}$ system; C_{Radi} is the cost of the RadiCold subsystem, including the cost of RadiCold module, pump, tank, cooling coil, and pipe network; C_{RSAC} is the cost of the RSAC in $RadiCold_{hc}$ system; and C_{SACL} is the cost of the SACL.

In Eq. (15), "$C_{\text{Radi}} + C_{\text{RSAC}}$" is the total cost of $RadiCold_{hc}$ system, and "C_{SACL}" indicates the total cost of SACL, a currently common air conditioning system in single-family houses. Thus, "$C_{\text{Radi}} + C_{\text{RSAC}}$-$C_{\text{SACL}}$" is also the incremental cost of $RadiCold_{hc}$ system compared to SACL. Then the *SPP* calculated here is the payback period of the incremental cost of the $RadiCold_{hc}$ system over SACL.

3.3. Cost of components in the $RadiCold_{hc}$ system

The cost of the RadiCold module comprises the cost of the radiative film and the polycarbonate panel. The retail price of polycarbonate panel is about \$22/m^2 [52]. The radiative film based on the novel randomized glass-polymer hybrid metamaterial is made from low-cost roll-to-roll manufacturing. The cost of the RadiCold module is estimated at \$25/m^2 in this work. For the $RadiCold_{hc}$ system pipe network, the main pipe (including supply pipe and return pipe) length is estimated at 12 m that counts in the height of the house, and the branch pipe connected to each RadiCold module is estimated at 2 m. Then we can estimate the major component cost of the $RadiCold_{hc}$ system according to [51], as listed in Table 4. The electricity prices found from EIA [53] are \$0.12/kWh for Orlando, \$0.19/kWh for San Diego, \$0.19/kWh for San Francisco, and \$0.12/kWh for Denver.

4. Results and discussion

4.1. Example case of $RadiCold_{hc}$ system optimization

In this section, an example of applying $RadiCold_{hc}$ system to the single-family house in Orlando, FL based on the TMY3 weather data [54] has been given to demonstrate the optimization process. With the average hourly cooling load of the design day (i.e., July 21st for Orlando) calculated by EnergyPlus, the initial number of RadiCold modules is calculated by Eq. (13), and gives 31. The relationship between the *SPP* and the number of RadiCold modules is shown in Fig. 7. When the number of RadiCold modules is reduced to 26, the calculated *SPP* is 7.95 years, lower than the *ASPP* of 8 years. Then 26 RadiCold modules are obtained for the optimized size of RadiCold subsystem.

Following the optimization sizing process shown in Fig. 6, the numbers of RadiCold modules for all four locations have been optimized and the sizes of the RadiCold subsystem are summarized in Table 5.

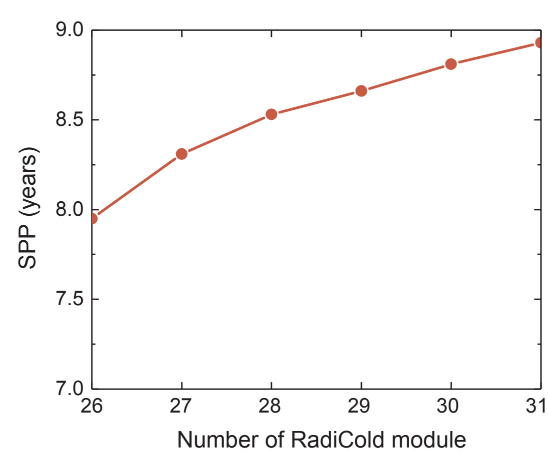

Fig. 7. Relationship between *SPP* and the number of RadiCold modules for Orlando.

Table 5
Sizes of optimized RadiCold subsystems for four locations.

No	Location	Number of RadiCold modules	Tank volume (m^3)
1	Orlando	26	1.30
2	San Diego	15	0.75
3	San Francisco	6	0.30
4	Denver	11	0.55

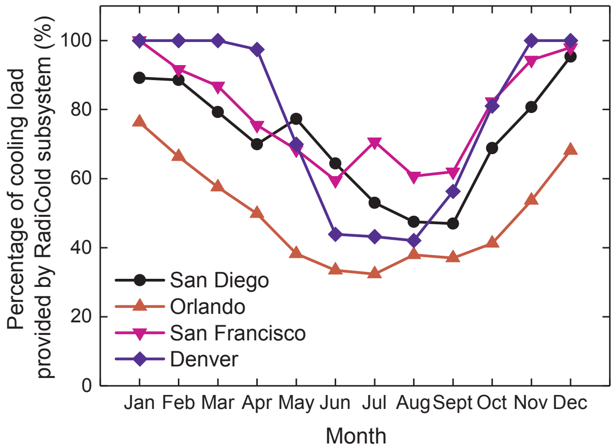

Fig. 8. Monthly percentage of cooling load covered by the RadiCold subsystem.

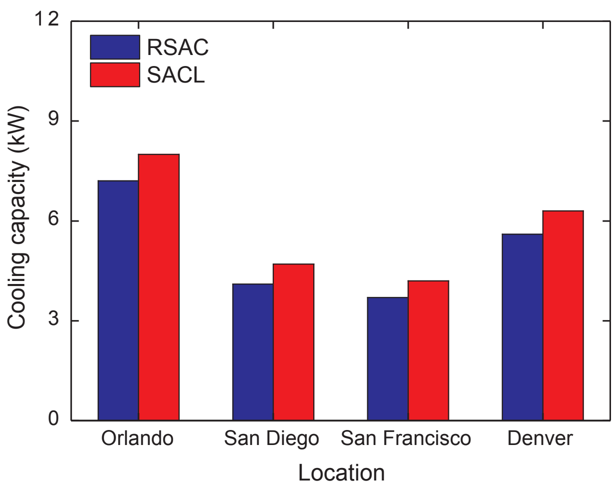

Fig. 9. Cooling capacity of the SACL and the RSAC for four locations.

4.2. Cooling benefit of the RadiCold$_{hc}$ system

The monthly percentage of cooling load covered by the RadiCold subsystem is shown in Fig. 8. Compared to the SACL, the overall annual cooling load addressed by the RadiCold subsystem is 40.9% in Orlando, 60.6% in San Diego, 68.1% in San Francisco, and 51.9% in Denver. The cold energy from the RadiCold subsystem is generated by the radiative cooling surface, a kind of "free" cooling energy. As shown in Fig. 8, the percentage of free cooling energy (i.e., cooling energy addressed by the RadiCold subsystem) is lower in summer, when there is a higher cooling load and a relatively lower radiative cooling power output. In contrast, the free cooling energy provided by the RadiCold subsystem in the cold 5 months (November to March) is higher than 53.7% for all four locations. In the typical cooling season (June to September), the free cooling energy covers about 32.4–38.0% of the cooling load in Orlando, 47.0–64.4% of the cooling load in San Diego, 59.5–70.7% of the cooling load in San Francisco, and 42.1–56.3% of the cooling load in Denver.

To determine the cooling capacities of the SACL and the RSAC, the

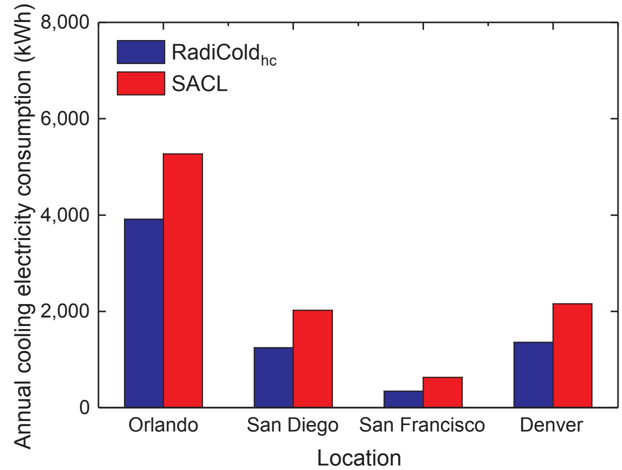

Fig. 10. Annual electricity consumption of the SACL and the RadiCold$_{hc}$ system.

peak cooling demand is used [55]. Compared to the SACL, the RSAC's cooling capacity is evaluated in the RadiCold$_{hc}$ system due to partial cooling loads addressed by the free cooling energy from the RadiCold subsystem. As shown in Fig. 9, the cooling capacities of the SACL and the RSAC of the RadiCold$_{hc}$ system are 8.0 kW and 7.2 kW in Orlando, 4.7 kW and 4.1 kW in San Diego, 4.2 kW and 3.7 kW in San Francisco, and 6.3 kW and 5.6 kW in Denver, respectively. The cooling capacity of the RSAC is reduced by 10.0–12.8%, which economically benefits the RadiCold$_{hc}$ system as it will reduce the incremental cost of the system.

4.3. Cooling electricity saving potential

The most direct benefit of the RadiCold$_{hc}$ system is saving cooling electricity consumption. Fig. 10 shows the comparison of the annual cooling electricity consumption between the SACL and the RadiCold$_{hc}$ system for all four locations.

As shown in Fig. 10, the annual cooling electricity consumed by the RadiCold$_{hc}$ system is lower than the conventional SACL. For the RadiCold$_{hc}$ system, the annual cooling electricity saving is about 1355 kWh in Orlando, 779 kWh in San Diego, 288 kWh in San Francisco, and 799 kWh in Denver, resulting a reduction of 25.7%, 38.5%, 45.8%, and 37.1% respectively compared to the SACL in these four locations. In the cooling season (June to September), the average monthly cooling electricity consumption of the RadiCold$_{hc}$ system is about 599.5 kWh in Orlando, 225.7 kWh in San Diego, 63.4 kWh in San Francisco, and 299.0 kWh in Denver, in which the circulation pump in the RadiCold subsystem consumes 21.8 kWh, 8.4 kWh, 2.4 kWh, and 7.6 kWh respectively (Fig. 11). The circulation pump in the RadiCold subsystem is the only electricity consuming component. According to the monthly cooling electricity consumption shown in Fig. 11, the average annual coefficients of performance (COP$_a$) for the RadiCold$_{hc}$ systems are given in Table 6. Compared to the COP of the SACL system that is derived from EnergyPlus simulation, the COP$_a$ is increased more than 39.4% for the RadiCod$_{hc}$ system which incorporates a reduced-size split air conditioner.

4.4. Techno-economic analysis

Using Eq. (15), the simple payback periods are calculated at 8.0 years in Orlando, 4.8 years in San Diego, 7.3 years in San Francisco, and 7.5 years in Denver. These simple payback periods are estimated based on the costs specified in section 3.3. It is possible that these cost estimates could be significantly reduced with mass production of the RadiCold$_{hc}$ system.

Another economic analysis method to evaluate the maximum

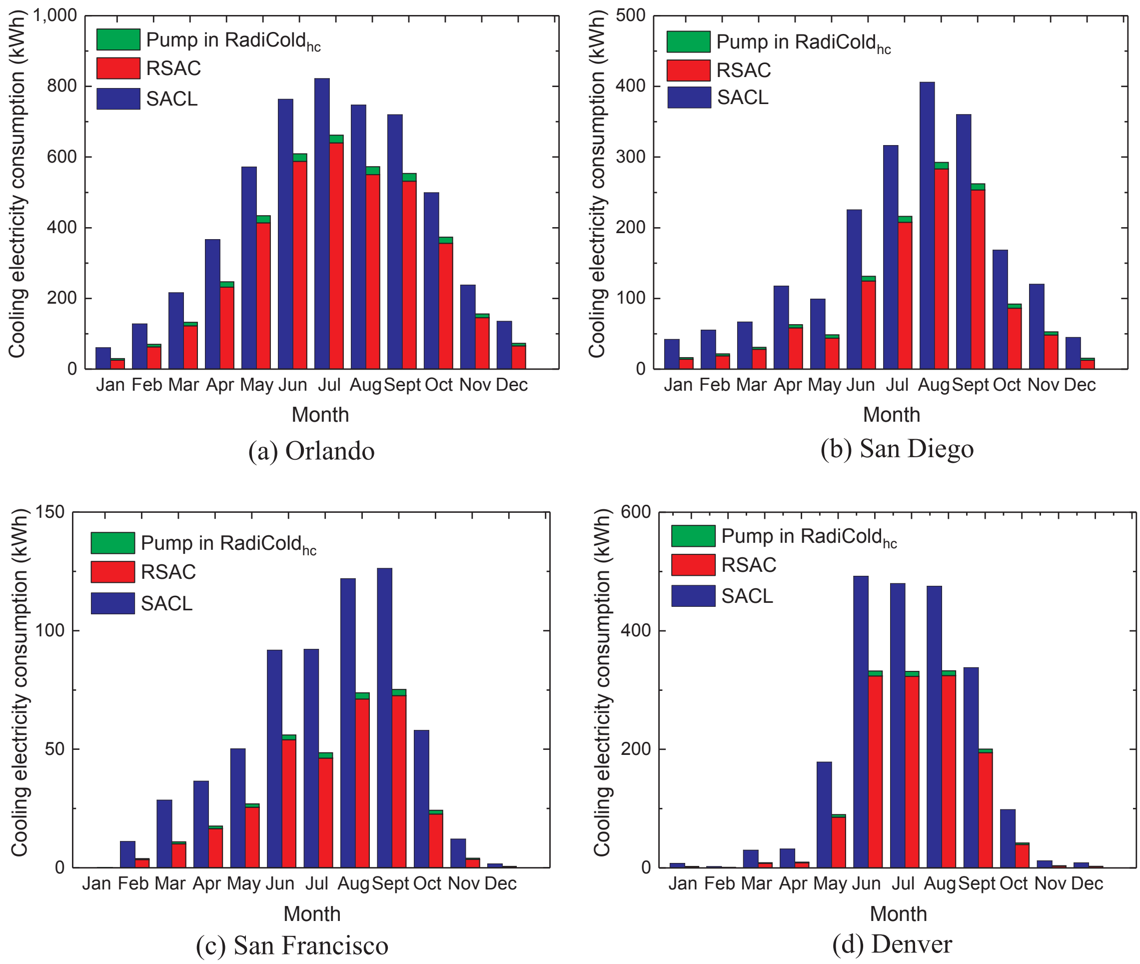

Fig. 11. Monthly cooling electricity consumption.

Table 6
Average annual coefficient of performance (COP_a).

Location	COP_a of the RadiCod$_{hc}$ system	COP_a of the SACL system modelled in EnergyPlus
Orlando	4.6	3.3
San Diego	5.7	3.2
San Francisco	6.5	3.2
Denver	5.0	3.2

acceptable incremental cost of the radiative cooling system has been proposed by Fernandez et al. [4],

$$AIC_{\max} = \frac{(E_{SACL}-E_{Radi-hc})P_E SPP}{A_S} \tag{16}$$

where AIC_{max} is the maximum acceptable incremental cost per unit size (e.g., m^2) of RadiCold module (i.e., the maximum acceptable incremental cost for employing RadiCold$_{hc}$ with a given SPP).

From Eq. (16), a lower AIC_{max} means the project is typically not desirable for investment position, but a higher AIC_{max} is preferred. As shown in Fig. 12, the maximum acceptable incremental costs for the RadiCold$_{hc}$ system with a simple payback period of 5-year are \$31.3/m^2 in Orlando, \$49.3/m^2 in San Diego, \$45.6/m^2 in San Francisco, and \$43.6/m^2 in Denver. Furthermore, the maximum acceptable incremental costs will increase to \$50.0/m^2 in Orlando, \$78.9/m^2 in San Diego, \$73.0/m^2 in San Francisco, and \$69.7/m^2 in Denver for the 8-year simple payback period. These maximum acceptable incremental costs of the modelled RadiCold$_{hc}$ systems are relatively high for

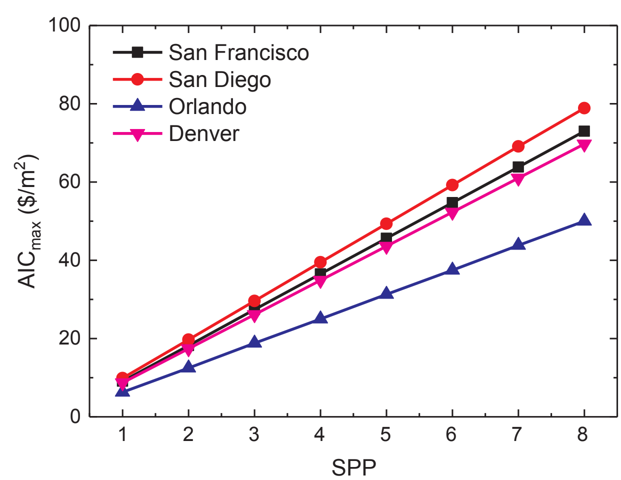

Fig. 12. Maximum acceptable incremental costs of the RadiCold$_{hc}$ system for four locations.

radiative cooling technology [4], indicating RadiCold$_{hc}$ system is a cost effective energy efficiency measure for application in residential buildings.

In summary, when applying a RadiCold$_{hc}$ system to a residential building, three steps should be done: (1) pre-size the RadiCold subsystem by quantifying the number of RadiCold modules according to Eq. (13); (2) design of the RadiCold$_{hc}$ system using EnergyPlus based optimization process as described above; and (3) construction of the

RadiCold$_{hc}$ system based on the optimized design.

There are wide applications of the recently developed novel radiative cooling metamaterial in buildings. For example, the metamaterial could be manufactured for cool roof application and can be used to generate cold water for integrating with air conditioning systems. As the first study, this work analyzes the energy saving potential and economic feasibility of the proposed RadiCold$_{hc}$ system in single-family houses based on EnergyPlus simulation. In future work, experimental tests to a prototype RadiCold$_{hc}$ system in a full-scale single-family house will be done to further validate the proposed system sizing method, the operation modes, and the simulation results.

5. Conclusion

A new hybrid radiative cooled-cold storage cooling system has been proposed in this work based on a recently developed novel radiative cooling metamaterial. This is the very first study on this radiative cooling metamaterial to provide cost-effective diurnal cooling to residential buildings. The proposed hybrid radiative cooled-cold storage cooling system can be conveniently integrated with the conventional air conditioning system in single-family houses. Three potential operating modes and a method to optimize the size of the hybrid radiative cooled-cold storage cooling system based on a threshold of 8-year simple payback period are introduced for the first time. The main conclusions that can be drawn from this study are the followings:

- Adoption of the hybrid radiative cooled-cold storage cooling system to a single-family house could save annual cooling electricity consumption by 25.7% in Orlando, FL, 38.5% in San Diego, CA, 45.8% in San Francisco, CA, and 37.1% in Denver, CO, and the corresponding simple payback period gives 8.0 years in Orlando, FL, 4.8 years in San Diego, CA, 7.3 years in San Francisco, CA, and 7.5 years in Denver, CO.
- Compared to the coefficient of performance of the split air conditioner lonely system, the average annual coefficient of performance of the hybrid radiative cooled-cold storage cooling system is increased by more than 39.4%.
- As an economically feasible cooling system, the maximum acceptable incremental costs of the hybrid radiative cooled-cold storage cooling system are \$50.0/m^2 in Orlando, FL, \$78.9/m^2 in San Diego, CA, \$73.0/m^2 in San Francisco, CA, and \$69.7/m^2 in Denver, CO for the 8-year simple payback period.

Acknowledgement

This research is financially supported by the U.S. Department of Energy's Advanced Research Projects Agency-Energy (ARPA-E) grant DE-AR0000580.

Appendix A

See Table A1.

Table A.1
Monthly cooling energy provided and cooling electricity consumption.

Month	San Diego, CA		Orlando, FL		San Francisco, CA		Denver, CO	
	Cooling energy (MJ)	Cooling electricity consumption (kWh) SACL/RadiCold$_{hc}$	Cooling energy (MJ)	Cooling electricity consumption (kWh) SACL/RadiCold$_{hc}$	Cooling energy (MJ)	Cooling electricity consumption (kWh) SACL/RadiCold$_{hc}$	Cooling energy (MJ)	Cooling electricity consumption (kWh) SACL/RadiCold$_{hc}$
Jan	514.6	42.1/16.2	753.2	60.7/29.8	0.3	0.02/0.04	97.0	7.7/2.4
Feb	693.0	55.2/21.6	1545.9	127.8/70.1	138.6	11.1/3.9	31.4	2.5/0.9
Mar	831.3	66.7/31.0	2620.2	216.1/132.7	355.6	28.5/11.0	366.7	30.0/8.9
Apr	1453.3	117.5/62.8	4468.8	366.8/246.8	455.9	36.6/17.6	384.8	32.0/9.9
May	1267.4	99.2/48.5	6920.7	572.4/434.1	615.7	50.2/26.9	2061.5	178.7/89.9
Jun	2882.9	225.5/131.5	9385.5	763.4/609.2	1147.2	91.8/56.0	5423.4	492.3/332.0
Jul	4092.8	316.5/216.2	10099.8	822.2/662.0	1179.8	92.1/48.5	5392.5	479.8/331.5
Aug	5186.6	405.8/292.7	9260.0	747.1/572.8	1543.6	122.0/73.8	5338.7	475.3/332.4
Sept	4610.1	360.1/262.3	8820.5	720.0/553.8	1621.8	126.2/75.2	3806.0	338.0/200.3
Oct	2138.4	168.6/92.1	6220.5	499.2/373.6	716.5	57.9/24.2	1173.9	98.3/42.0
Nov	1479.3	120.0/52.9	2960.7	238.1/155.9	152.7	12.1/4.1	151.5	12.1/3.7
Dec	551.5	45.1/15.5	1668.3	135.2/72.8	21.2	1.7/0.6	108.6	8.8/2.7

References

[1] Zhao D, Martini CE, Jiang S, Ma Y, Zhai Y, Tan G, et al. Development of a single-phase thermosiphon for cold collection and storage of radiative cooling. Appl Energy 2017;205:1260–9.
[2] Lu X, Xu P, Wang H, Yang T, Hou J. Cooling potential and applications prospects of passive radiative cooling in buildings: the current state-of-the-art. Renew Sustain Energy Rev 2016;65:1079–97.
[3] Hossain MM, Gu M. Radiative cooling: principles, progress, and potentials. Adv Sci 2016;3:1500360.
[4] Fernandez N, Wang W, Alvine KJ, Katipamula S. Energy savings potential of radiative cooling technologies. Pacific Northwest National Laboratory (PNNL), Richland, WA (US); 2015.
[5] Michell D, Biggs KL. Radiation cooling of buildings at night. Appl Energy 1979;5:263–75.
[6] Orel B, Gunde MK, Krainer A. Radiative cooling efficiency of white pigmented paints. Sol Energy 1993;50:477–82.
[7] Spanaki A, Kolokotsa D, Tsoutsos T, Zacharopoulos I. Assessing the passive cooling effect of the ventilated pond protected with a reflecting layer. Appl Energy 2014;123:273–80.
[8] Cotana F, Rossi F, Filipponi M, Coccia V, Pisello AL, Bonamente E, et al. Albedo control as an effective strategy to tackle Global Warming: a case study. Appl Energy 2014;130:641–7.
[9] Hu M, Pei G, Wang Q, Li J, Wang Y, Ji J. Field test and preliminary analysis of a combined diurnal solar heating and nocturnal radiative cooling system. Appl Energy 2016;179:899–908.
[10] Granqvist CG, Hjortsberg A. Radiative cooling to low temperatures: general considerations and application to selectively emitting SiO films. J Appl Phys 1981;52:4205–20.
[11] Addeo A, Nicolais L, Romeo G, Bartoli B, Coluzzi B, Silvestrini V. Light selective structures for large-scale natural air-conditioning. Sol Energy 1980;24:93–8.
[12] Harrison A, Walton M. Radiative cooling of TiO_2 white paint. Sol Energy 1978;20:185–8.
[13] Nilsson TM, Niklasson GA, Granqvist CG. A solar reflecting material for radiative cooling applications: ZnS pigmented polyethylene. Sol Energy Mater Sol Cells 1992;28:175–93.
[14] Nilsson TMJ, Niklasson GA. Radiative cooling during the day-simulations and experiments on pigmented polyethylene cover foils. Sol Energy Mater Sol Cells 1995;37:93–118.

[15] Goldstein EA, Raman AP, Fan S. Sub-ambient non-evaporative fluid cooling with the sky. Nat Energy 2017;2:17143.
[16] Wang W, Fernandez N, Katipamula S, Alvine K. Performance assessment of a photonic radiative cooling system for office buildings. Renew Energy 2018;118:265–77.
[17] Zhai Y, Ma YG, David SN, Zhao DL, Lou RN, Tan G, et al. Scalable-manufactured randomized glass-polymer hybrid metamaterial for daytime radiative cooling. Science 2017;355:aai7899.
[18] Spanaki A, Kolokotsa D, Tsoutsos T, Zacharopoulos I. Theoretical and experimental analysis of a novel low emissivity water pond in summer. Sol Energy 2012;86:3331–44.
[19] Spanaki A, Tsoutsos T, Kolokotsa D. On the selection and design of the proper roof pond variant for passive cooling purposes. Renew Sustain Energy Rev 2011;15:3523–33.
[20] Ali AHH. Passive cooling of water at night in uninsulated open tank in hot arid areas. Energy Convers Manage 2007;48:93–100.
[21] Tang R, Etzion Y. On thermal performance of an improved roof pond for cooling buildings. Build Environ 2004;39:201–9.
[22] Raeissi S, Taheri M. Skytherm: an approach to year-round thermal energy sufficient houses. Renew Energy 2000;19:527–43.
[23] Tevar JAF, Castaño S, Marijuán AG, Heras MR, Pistono J. Modelling and experimental analysis of three radioconvective panels for night cooling. Energy Build 2015;107:37–48.
[24] Okoronkwo CA, Nwigwe KN, Ogueke NV, Anyanwu EE, Onyejekwe DC, Ugwuoke PE. An experimental investigation of the passive cooling of a building using nighttime radiant cooling. Int J Green Energy 2014;11:1072–83.
[25] Hosseinzadeh E, Taherian H. An experimental and analytical study of a radiative cooling system with unglazed flat plate collectors. Int J Green Energy 2012;9:766–79.
[26] Anderson T, Duke M, Carson J. Performance of an unglazed solar collector for radiant cooling; 2013.
[27] Hollick J. Nocturnal radiation cooling tests. Energy Proc 2012;30:930–6.
[28] Bagiorgas HS, Mihalakakou G. Experimental and theoretical investigation of a nocturnal radiator for space cooling. Renew Energy 2008;33:1220–7.
[29] Mihalakakou G, Ferrante A, Lewis JO. The cooling potential of a metallic nocturnal radiator. Energy Build 1998;28:251–6.
[30] Khedari J, Waewsak J, Thepa S, Hirunlabh J. Field investigation of night radiation cooling under tropical climate. Renew Energy 2000;20:183–93.
[31] Zhang S, Niu J. Cooling performance of nocturnal radiative cooling combined with microencapsulated phase change material (MPCM) slurry storage. Energy Build 2012;54:122–30.
[32] Eicker U, Dalibard A. Photovoltaic–thermal collectors for night radiative cooling of buildings. Sol Energy 2011;85:1322–35.
[33] Zhao B, Hu M, Ao X, Pei G. Conceptual development of a building-integrated photovoltaic-radiative cooling system and preliminary performance analysis in Eastern China. Appl Energy 2017;205:626–34.
[34] Collins T, Parker S. Technology Installation Review: WhiteCap Roof Spray Cooling System. Pacific Northwest National Laboratory, Richland, WA Accessed October; 1998; 23: 2015.
[35] Parker DS. Theoretical evaluation of the NightCool nocturnal radiation cooling concept. Submitted to: US Department of Energy FSEC-CR-1502-05; 2005.
[36] Rephaeli E, Raman A, Fan S. Ultrabroadband photonic structures to achieve high-performance daytime radiative cooling. Nano Lett 2013;13:1457–61.
[37] Raman AP, Anoma MA, Zhu L, Rephaeli E, Fan S. Passive radiative cooling below ambient air temperature under direct sunlight. Nature 2014;515:540–4.
[38] Zhu L, Raman A, Fan S. Color-preserving daytime radiative cooling. Appl Phys Lett 2013;103:223902.
[39] Zhu L, Raman A, Wang KX, Anoma MA, Fan S. Radiative cooling of solar cells. Optica 2014;1:32–8.
[40] Farzad M, O'neal DL. System performance characteristics of an air conditioner over a range of charging conditions. Int J Refrig 1991;14:321–8.
[41] U.S. Department of Energy. Engineering reference. US Department of Energy; 2016.
[42] Walton G. Passive solar extension of the building loads analysis and system thermodynamics (BLAST) program. United States Army Construction Engineering Research Laboratory, Champaign, IL. 1981; 40: 41.
[43] Walton GN. Thermal analysis research program reference manual. National Bureau of Standards, March; 1983.
[44] Bliss Jr RW. Atmospheric radiation near the surface of the ground: a summary for engineers. Sol Energy 1961;5:103–20.
[45] Clark G, Allen C. The estimation of atmospheric radiation for clear and cloudy skies. In: Proc 2nd National Passive Solar Conference (AS/ISES; 1978. p. 675–8.
[46] Berdahl P, Fromberg R. The thermal radiance of clear skies. Sol Energy 1982;29:299–314.
[47] Berdahl P, Martin M. Emissivity of clear skies. Sol Energy 1984;32:663–4.
[48] Martin M, Berdahl P. Characteristics of infrared sky radiation in the United States. Solar Energy 1984;33:321–36.
[49] Berger X, Buriot D, Garnier F. About the equivalent radiative temperature for clear skies. Sol Energy 1984;32:725–33.
[50] Online source, retrieved on September 28, 2017, < https://www.energycodes.gov/development/residential > .
[51] Gordian RSMeans Data. Building construction costs with rsmeans data. Gordian RSMeans Data; 2017.
[52] Online source, retrieved on September 28, 2017, < https://www.amazon.com/Easy-Ship-clear-Twinwall-Polycarbonate/dp/B013XIVCNY/ref=sr_1_4?ie=UTF8&qid=1504572921&sr=8-4&keywords=polycarbonate > .
[53] Online source, retrieved on September 28, 2017, < https://www.eia.gov/electricity/monthly/epm_table_grapher.cfm?t=epmt_5_06_a > .
[54] Online source, retrieved on September 28, 2017, < https://energyplus.net/weather-region/north_and_central_america_wmo_region_4/USA%20%20 > .
[55] ASHRAE Standard Committee. ASHRAE handbook: Fundamentals; 2013.